
Supplementary Information

Ternary Heterogeneous Pt-Ni-Au Nanowires with Enhanced Activity and Stability for PEMFC

Zhicheng Lin,[a] Yuan Sheng,[a] Jia Li,[a] Zhiyan Rui,[a] Yide Liu,[a] Jianguo Liu*[ab] and Zhigang Zou [ab]

a. Jiangsu Key Laboratory for Nano Technology, National Laboratory of Solid State Microstructures, College of Engineering and Applied Sciences, and Collaborative Innovation Center of Advanced Microstructures, Nanjing University, 22 Hankou Road, Nanjing, 210093, China. E-mail: jianguoliu@nju.edu.cn

b. Kunshan Sunlaite New Energy Co,. Ltd., 1666 South Zuchongzhi Road, Kunshan 215347, Jiangsu, China

Preparation of Pt-Ni-Au NWs

The nanowires were fabricated via a modulated solvothermal method. Generally, 535 μL H_2PtCl_6 (0.038 M), 500 mg KOH, and 2 mg $Ni(acac)_2$ were added to the mixed solution of 4 mL EG and 6 mL DMF. After stirring for 12 h, additional 290 μL $HAuCl_4$ (0.024 M) was added to the homogenous solution to blend for 12 h. Then, the mixture was then transferred to a 20 mL Teflon-lined autoclave to react at 180 °C for 8 h, and cooled down to room temperature naturally. The product was collected by centrifugation and washed with a mixed solution of deionized water and ethanol several times.

Preparation of Pt-Ni NWs

The Pt-Ni NWs were synthesized following the same synthesizing process of Pt-Ni-Au NWs, but with the absence of $HAuCl_4$.

Preparation of Pt-Au NWs

The Pt-Au NWs were synthesized following the same synthesizing process of Pt-Ni-Au NWs, but with the absence of $Ni(acac)_2$.

Carbon supporting of NWs

A specific amount of water was filled in a beaker containing 150 mg XC-72R and, was ultrasonically blended for 10 min. After adding the synthesized NWs to the carbon solution, the mixture was stirred for at least 8 h. The mixture was then filtered and washed 3 times with a mixture of water and ethanol before drying in vacuum oven at 60 °C overnight.

Physical characterization

Structural information was obtained via transmission electron microscopy (TEM) and highresolution transmission electron microscopy (HRTEM) on TECNAI G2 FEI. High-angle annular dark-field scanning transmission electron microscopy (HAADF-STEM) and energy-dispersive X-ray spectroscopy (EDS) were conducted on TALOS F200X operating at 200 kV. Powder X-ray diffraction (PXRD, ARL-9800) and, Cu Kα radiation monochromatizing, was used to detect the crystal structure. X-ray photoelectron spectroscopy (XPS, PHI 5000 VersaProbe) was employed to characterize the surface elements information. Accurate metal loading was confirmed by inductively coupled plasma optical emission spectrometry (ICP-OES, Optima 5300DV).

Electrochemical measurement

The electrochemical characterizations were performed in a three-electrode system using CHI760e. A glassy carbon (GC) electrode served as the working electrode, reversible hydrogen electrode (RHE) as the reference electrode, and a graphite rod as the counter electrode. 5 mg catalyst was dispersed in a 2 mL solution composed of 1.8 mL ethanol, 180 μL ultrapure water and 20 μL 5 wt% Nafion. After ultrasonic blending for at least 30 min, the catalyst ink was cast onto the GC electrode (0.19625 cm^2) and, dried at ambient temperature. Pt loading on the GC electrodes was controlled at approximately 7 μg/cm^2.

Cyclic voltammetry (CV) experiments were conducted in 0.1 M $HClO_4$ saturated with N_2 at a sweep rate of 0.05 V s^{-1} from 0–1.2 V. Linear sweep voltammetry (LSV) was performed at a scan rate of 0.01 V s^{-1} at 1600 rpm in O_2 saturated 0.1 M $HClO_4$ solution. The accelerated durability test (ADT) was adopted for 0.1 M $HClO_4$ saturated with N_2, at a scanning rate of 0.1 V s^{-1} from 0.6 V–1.0 V for 30,000 cycles. All these experiments were conducted at 25 °C. In this work, unless stated, all potentials were relative to RHE.

Single-cell test

The as-synthesized Pt-Ni-Au NWs were used as cathodic catalysts to assess their single-cell performance. The tests were performed in SCRIBNER 850e. To prepare the catalytic slurry, the as-synthesized Pt-Ni-Au NWs and 5wt% Nafion were mixed in isopropanol by supersonic blending. Then, the prepared slurry was sprayed on one side of gas diffusion layer (GDL, SGL28BC) as cathode layer. Commercial Pt/C (JM, 60%) was sprayed on another GDL and, used as the anode layer. The as-prepared cathode layer, Nafion membrane (Dupont, 211), and anode layer were assembled to form the membrane assembly electrode (MEA). For comparison, another MEA was fabricated by a similar process, but using 60 wt% commercial Pt/C in cathode layer. The active area of MEA was 1 cm^2. The Pt loading of cathode was controlled at 0.1 mg cm^{-2}, and that of anode at 0.2 mg cm^{-2}.

In the single-cell test, pure hydrogen (200 sccm) and oxygen (200 sccm) were fed to anode and cathode, respectively. Both cell and gas humidifiers were maintained at 80 °C. No back pressure was exerted during the test. Accelerated durability test was adopted to evaluate the long-term stability of the catalyst according to the protocol of DOE: square wave between 0.6 V (3 s) and 0.95 V (3 s) was executed for 10,000 cycles. Throughout the ADT process, cathode gas was supplied by pure nitrogen (200 sccm)[a].

---

[a] DOE Fuel Cell Technologies Program Multi-Year Research, Development, and Demonstration Plan. 2016, 3.4-46.

Table S1. Atomic fraction of as-synthesized NWs according to ICP-OES.

	Pt	Ni	Au
Pt-Ni NWs	0.73	0.27	-
Pt-Ni-Au NWs	0.65	0.22	0.13

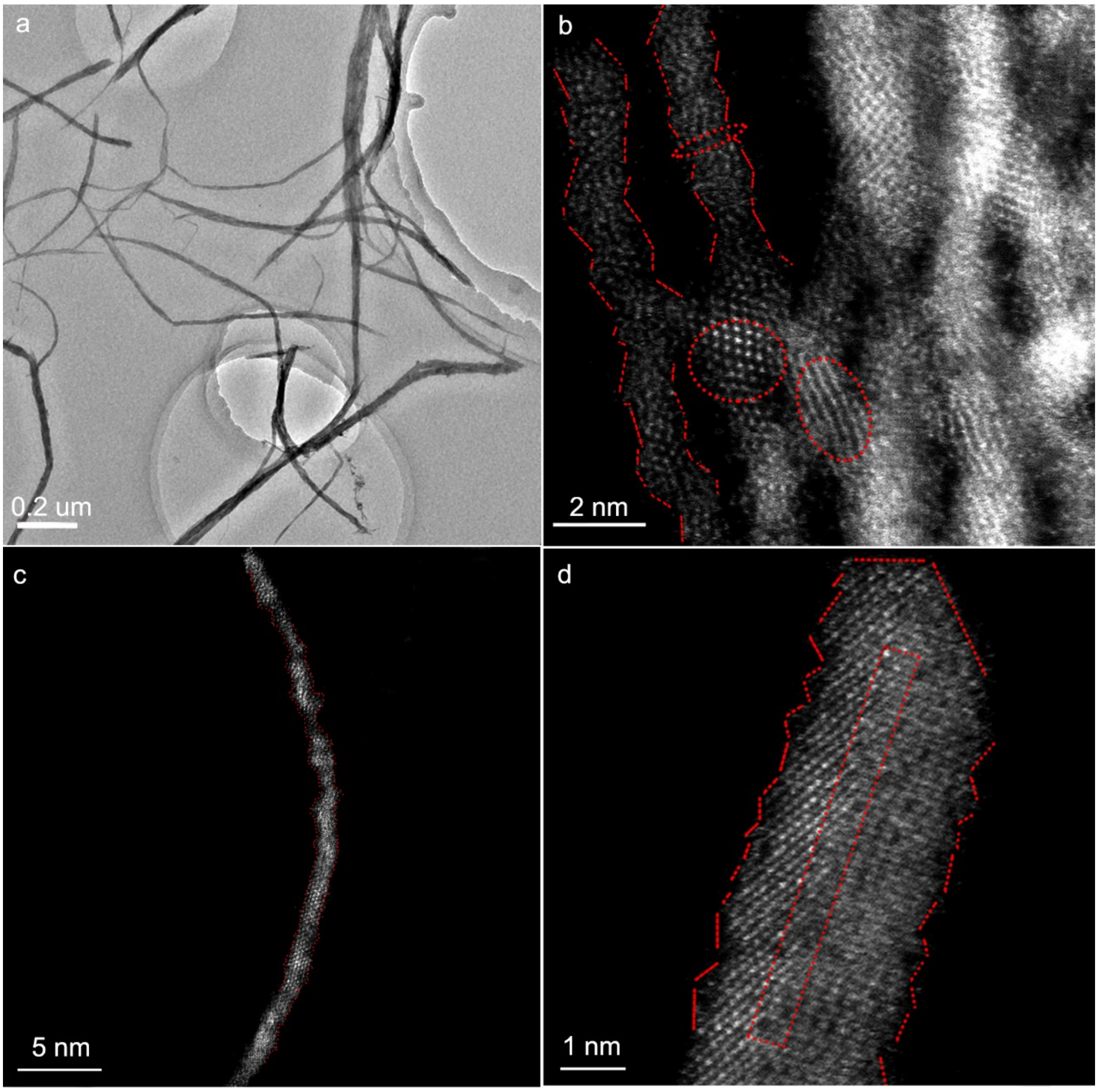

Fig. S1. Additional TEM images for Pt-Ni-Au NWs. (a) TEM images. (b-d) HAADF STEM images. Marks in (b-d) indicate rough surface, boundaries and deformation in Pt-Ni-Au NWs.

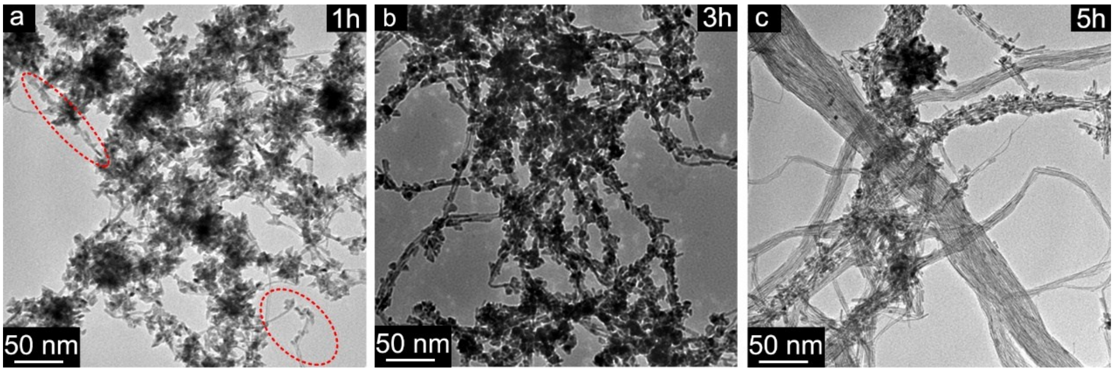

Fig. S2. Representative TEM images of intermediates after different reaction time. (a) after 1h, (b) after 3h and (c) after 5h. Cycles in (a) represent the outline of initial particles, aligning to wire-like shape.

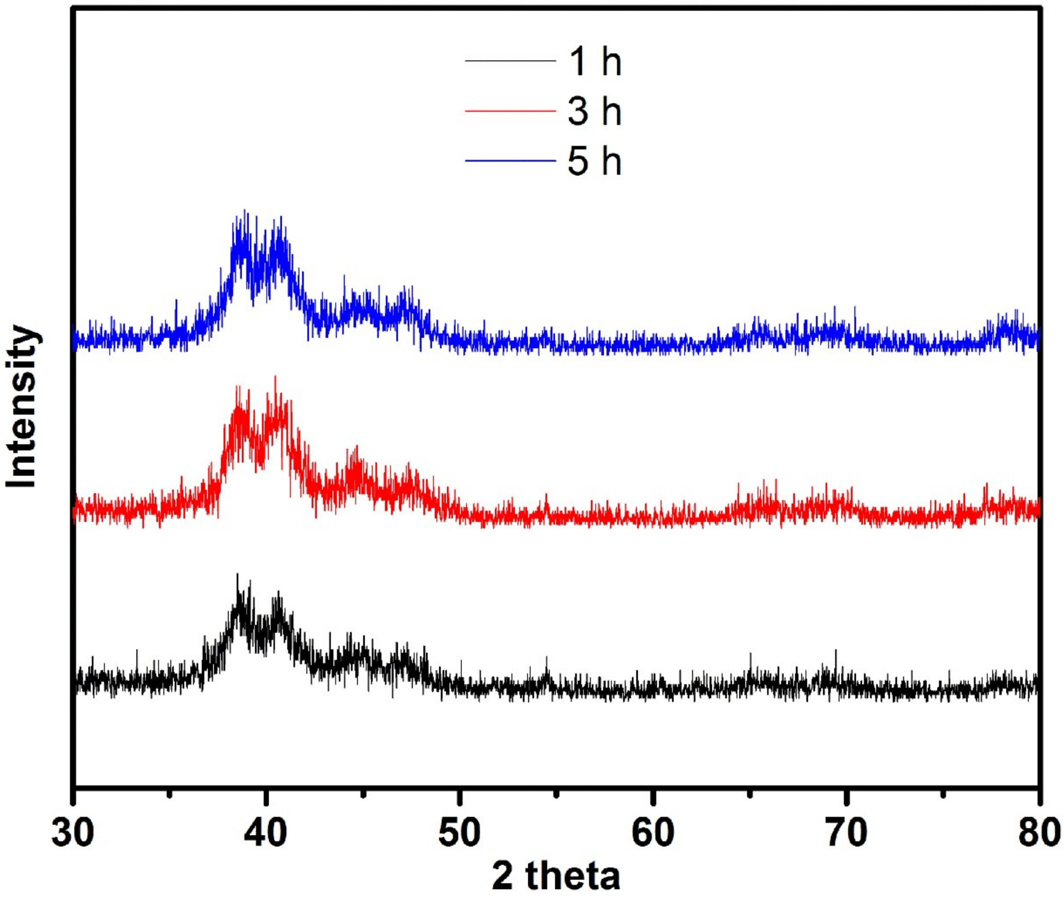

Fig. S3. XRD patterns of intermediates after different reaction time.

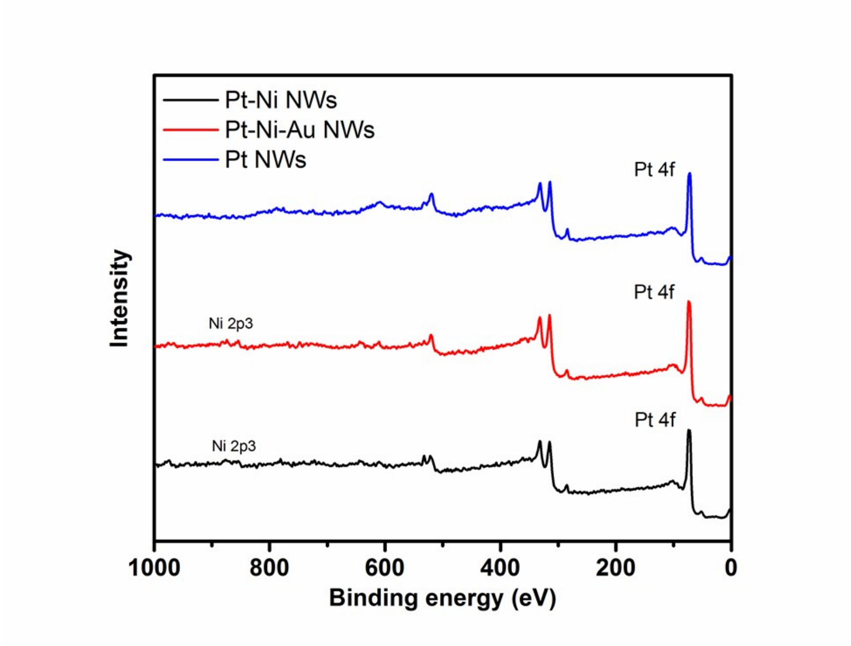

Fig. S4. XPS the survey spectrum of Pt NWs, Pt-Ni NWs and Pt-Ni-Au NWs.

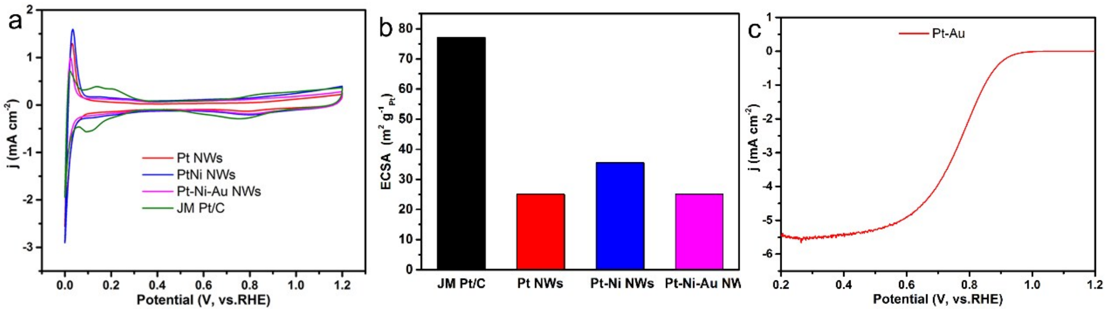

Fig. S5. (a) CV curves and (b) corresponding ECSA values of JM Pt/C, Pt NWs, Pt-Ni NWs and Pt-Ni-Au NWs. (c) LSV curve of Pt-Au NWs.

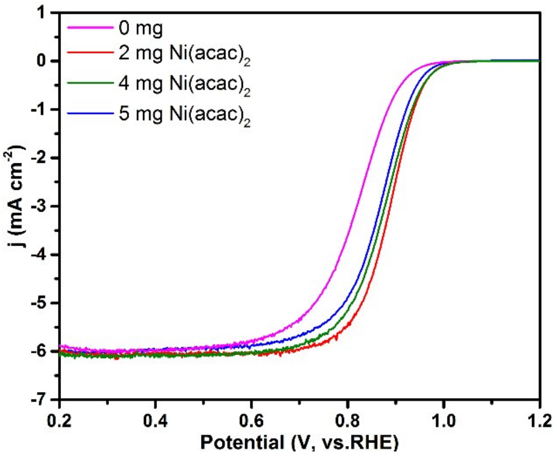

Fig.S6. LSV curves of Pt-Ni NWs with different amounts of $Ni(acac)_2$.

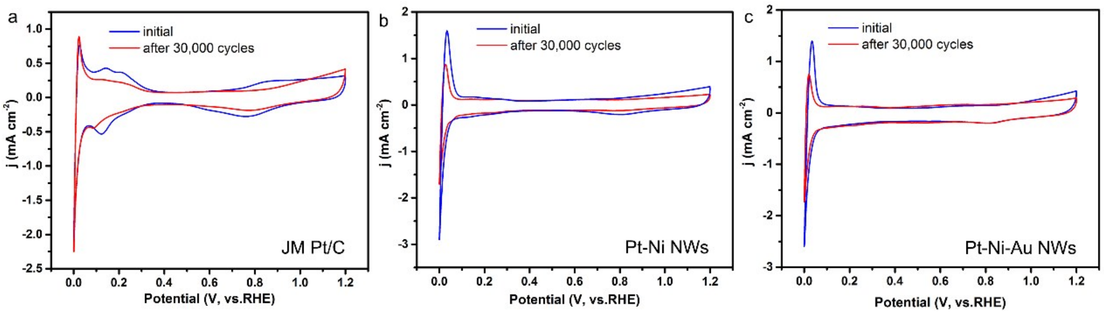

Fig.S7. CV curves before and after ADT cycling at 0.6–1.0 V in N_2 background with a scan rate of 0.1 V s^{-1}. (a) JM Pt/C, (b) Pt-Ni NWs, and (c) Pt-Ni-Au NWs.

Table S2. Changes of ECSA of Pt-Ni NWs and Pt-Ni-Au NWs before and after ADT

	Pt-Ni NWs	Pt-Ni-Au NWs
Initial (m^2 $g^{-1}{}_{Pt}$)	35.5	25.1
After 30,000 cycles (m^2 $g^{-1}{}_{Pt}$)	11.3	9.2

Table S3. Atomic fraction of Pt-Ni NWs before and after ADT

Pt-Ni NWs	Pt	Ni
Initial	0.73	0.27
After 30,000 cycles	0.86	0.14

The ratio after 30,000 cycles is according to the result of EDS.

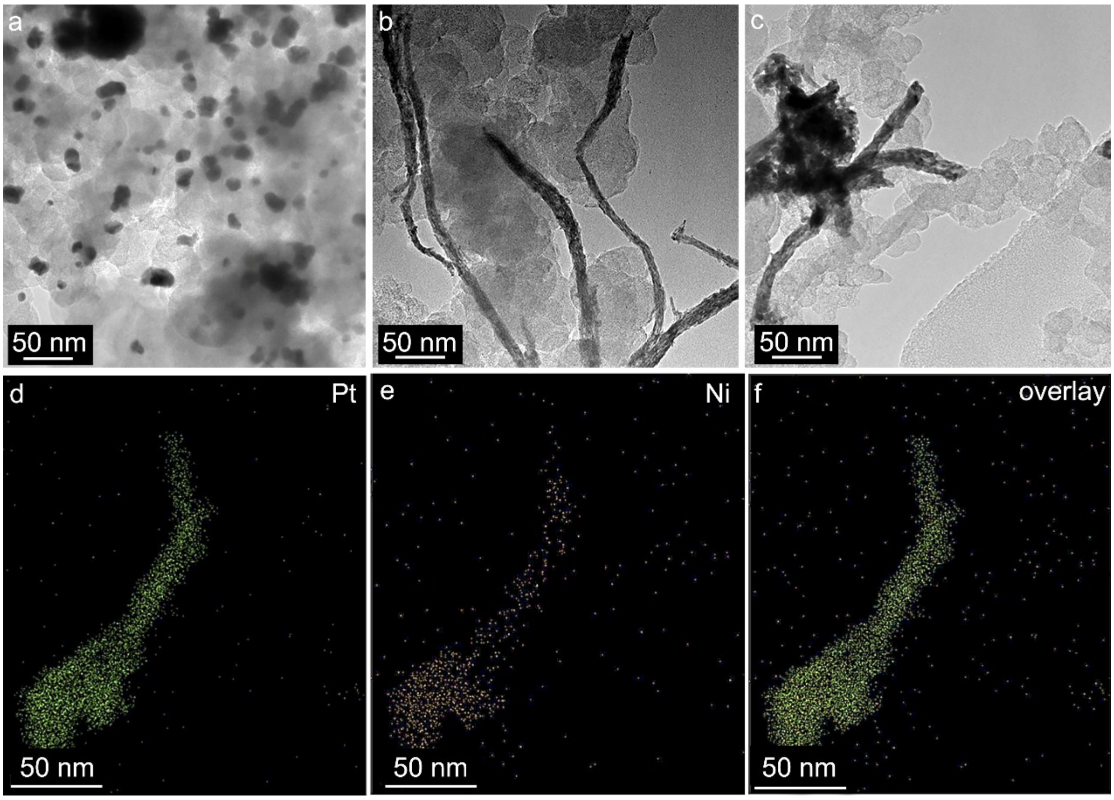

Fig. S8. Additional images of JM Pt/C and Pt-Ni NWs before and after 30,000 cycles from 0.6V–1.0 V at N_2 background. (a) JM Pt/C after 30,000 cycles, (b) Pt-Ni NWs initial, (c) Pt-Ni NWs after 30,000 cycles, (d-f) EDS mapping of Pt-Ni NWs after 30,000 cycles.

Table S4. Atomic fraction of Pt-Ni-Au NWs before and after ADT.

Pt-Ni-Au NWs	Pt	Ni	Au
initial	0.65	0.22	0.13
After 30,000 cycles	0.72	0.17	0.11

The ratio after 30,000 cycles is according to the result of EDS.

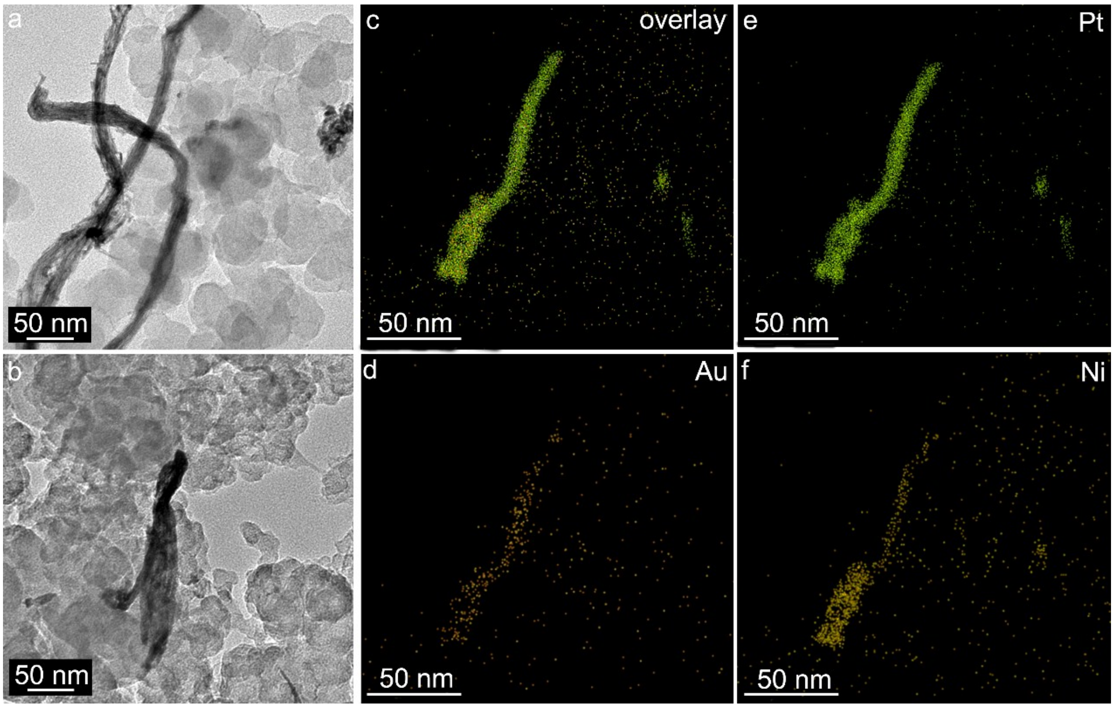

Fig. S9. Additional images of Pt-Ni-Au NWs before and after 30,000 cycles from 0.6V–1.0 V at N_2 background. (a) initial, (b) after 30,000 cycles, (c-f) EDS mapping after 30,000 cycles.